JOC The Journal of Organic Chemistry

Article

pubs.acs.org/joc

How the Bicyclo[4.1.0] Substrate Isomerizes into 4,5-Dihydrobenzo[*b*]furan: The Contribution from $W(CO)_5$ and NEt_3

Jingxi Wu, Mian Wang, Lisheng Wang, Jianyi Wang,* and Linbin Jiang*

School of Chemistry and Chemical Engineering, Guangxi University, Nanning 530004, People's Republic of China

Supporting Information

ABSTRACT: The cycloisomerization of a bicyclo[4.1.0] substrate into 4,5-dihydrobenzo[*b*]furan was investigated by using density functional theory (DFT). Comparative studies on four models (model I: with $W(CO)_5$ and NEt_3; model II: without NEt_3; model III: without $W(CO)_5$; model IV: without $W(CO)_5$ and NEt_3) indicate that this reaction is the most likely to proceed under model I to give the product. The ring closure process is greatly associated with the H1 and H2 transfer processes, because in the H1 transfer process, the carbene C3 atom is mainly stabilized by $W(CO)_5$, and in the H2 atom transfer process the C3 atom is mainly stabilized by the O1 atom. The rearrangement of **12** to give **14** is the rate-determining step of this reaction with a free energy barrier of 31.0 kcal/mol. The presence of $W(CO)_5$ can not only promote the H1 transfer and the ring closure (**1**→**6**-[**W**]) but can also be slightly favorable for the isomerization of **6**-[**W**] into **11**-[**W**](**6**-[**W**]→**11**-[**W**]). NEt_3 mainly has an effect in the **6**-[**W**]→**11**-[**W**] stage, in which it mainly plays proton-transfer bridge and proton-adsorption roles.

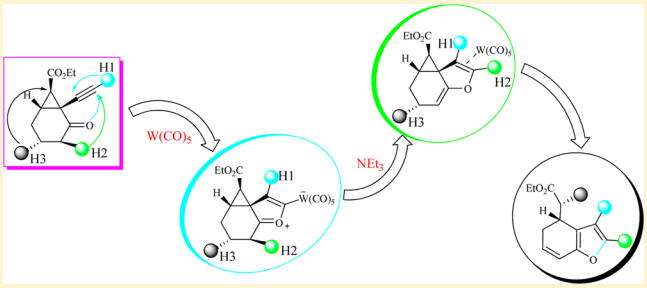

INTRODUCTION

Dihydrobenzofuran is a basic unit of many natural products and drugs and is a crucial pharmaceutical intermediate.[1,2] For example, the natural product pterocarpan, possessing a dihydrobenzofuran skeleton, shows a variety of biological activities, including antimicrobial, antitumor, antiulcer, etc.[3] A series of dihydrobenzofuran thiazolidine-2,4-diones are found to possess potential hypoglycemic activities.[4] A novel class of 2,3-dihydrobenzofuran-2-carboxylic acids were designed as highly potent and selective PPARα agonists.[5] Kadsurenone, possessing a dihydrobenzofuran unit, is considered as a competitive antagonist of the platelet activating factor (PAF) receptor.[6] Thus, the development of synthetic methods for dihydrobenzofurans is very significant for organic synthetic chemistry and medicinal chemistry.

In the past few decades, a variety of synthetic methods for dihydrobenzofurans have been reported.[7−15] For instance, the $Fe(ClO_4)_3$-catalyzed cycloaddition of a styrene to a quinone provides 2-(4-methoxy)phenyl-3-acetoxymethyl-2,3-dihydro-5-benzofuranol with high trans-selectivity (11:1).[16] The CuCl-catalyzed intramolecular cyclization of 2-(2′-chlorophenyl)-ethanol gives 4-chloro-2,3-dihydrobenzofuran with high selectivity (>92%).[17] The $Pd(OAc)_2$-catalyzed tandem reaction of 2-(3-methoxycarbonylallyloxyl)iodobenzene was used to construct a 3,3-disubstituted-2,3-dihydrobenzofuran.[18] Using AgOTf,[19] $Au(Cl)_3$,[20] $Rh_2(S\text{-}PTTEA)_4$,[21] $[Rh(COD)Cl]_2$,[22] and $Pd(dba)_2$[23] as the catalyst, diverse dihydrobenzofuran derivatives can also be successfully synthesized. However, the above catalysts are still not ideal for the synthesis of dihydrobenzofuran because of low yields and harsh reaction conditions.

Recently, an inexpensive tungsten complex $W(CO)_5$ was reported to catalyze the heterocycloisomerization of a bicyclo[4.1.0] substrate to afford a substituted 4,5-dihydrobenzo[*b*]furan under mild conditions in good yield,[24] shown in Scheme 1, attracting widespread attention from organic chemists. However, the CO ligand in the catalyst is toxic and highly flammable; therefore, optimization and redesign of the tungsten complex catalyst is required for the synthesis of dihydrobenzofuran. To accomplish this, it is first necessary to understand the catalytic mechanism of the tungsten complexes.

Scheme 1. Heterocycloisomerization of the Bicyclo[4.1.0] Substrate To Afford 4,5-Dihydrobenzo[*b*]furan

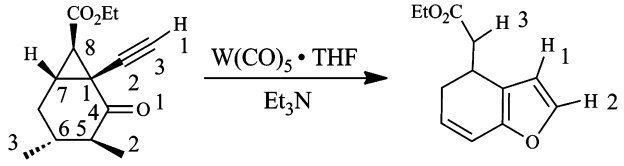

Several mechanisms activated by tungsten complexes have been theoretically investigated to date. For instance, the $(THF)W(CO)_5$-promoted cycloisomerization of 4-pentyn-1-ol has been studied by Sordo and co-workers.[25] They described the crucial role that THF plays in the catalytic reaction. Studies on $W(\equiv CMe)(R)_3$ (R═OMe, OCH_2F, NMe_2, Cl)-catalyzed

Received: August 15, 2013
Published: October 4, 2013

   dx.doi.org/10.1021/jo4017748 | J. Org. Chem. 2013, 78, 10812−10820

Scheme 2. Four Possible Pathways for the Cycloisomerization of the Bicyclo[4.1.0] Substrate into 4,5-Dihydrobenzo[*b*]furan

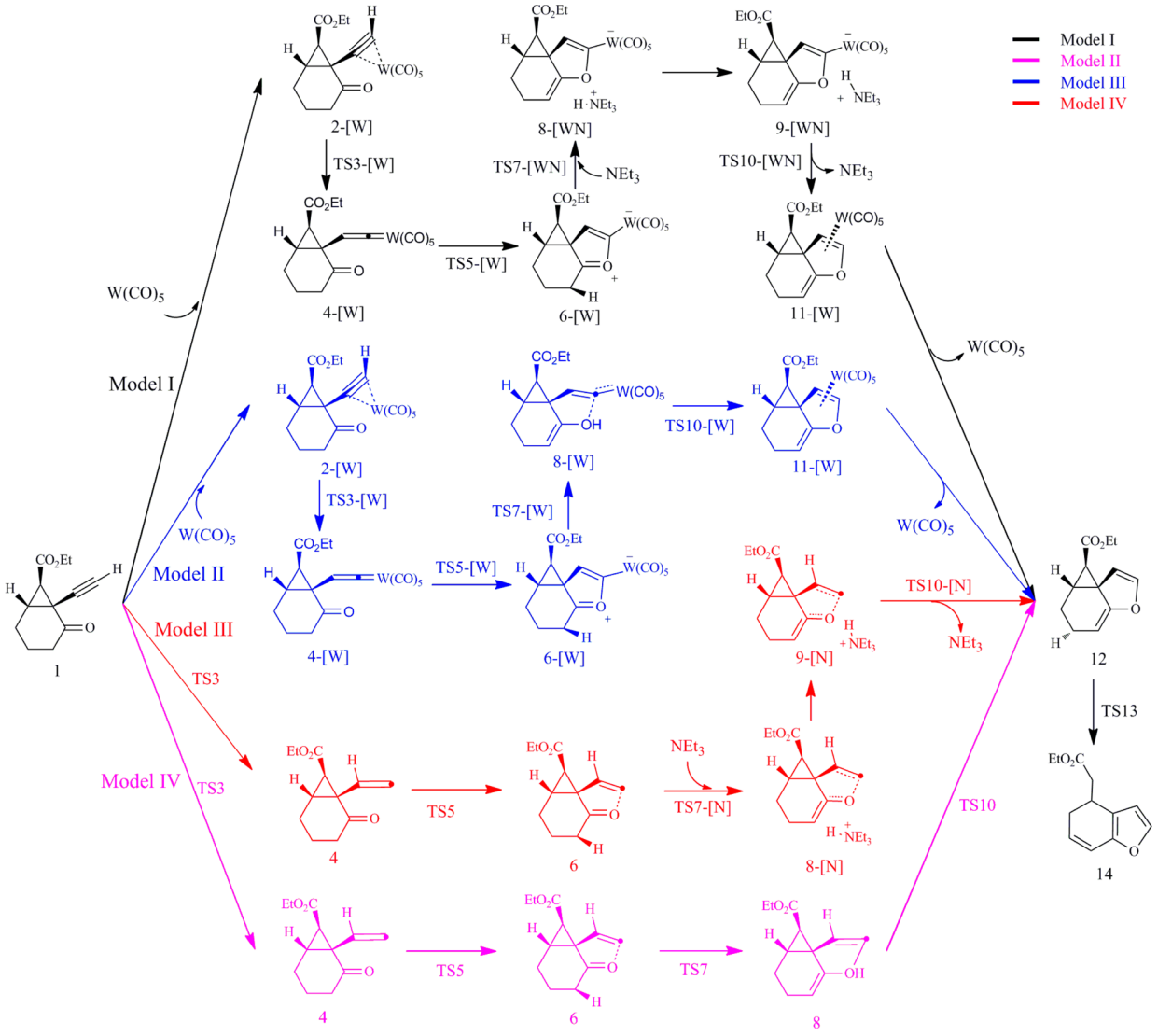

alkyne metathesis showed that alkoxide ligands with electron-withdrawing groups are likely to improve the activity of the catalyst.[26] The $W(CO)_5$-catalyzed cycloisomerization of 4-pentyn-1-ol was investigated by Morokuma and co-workers.[27] They deemed that the presence of $W(CO)_5$ is responsible for the regioselectivity. In addition, the formation of 2,2-dialkyldihydrobenzofurans catalyzed by $Pd(OAc)_2$ was studied by Fagnou and co-workers.[28] They revealed the reason why the formation of the C−C bond is not very dependent upon substrate stoichiometry. The formation of benzofuran with the intramolecular substitution of haloalkenes has been studied by Ando and co-workers,[29] and they deemed that the *E*-configuration substrate was more likely to afford the benzofuran in high yield when compared to the corresponding *Z*-configuration substrate. However, no theoretical investigation has been reported for the isomerization of a bicyclo[4.1.0] substrate into 4,5-dihydrobenzo[*b*]furan. The role of $W(CO)_5$ and NEt_3 in the reaction is still ambiguous.

Referring to the experimental proposals, four computational models are designed and comparatively investigated for the heterocycloisomerization of the bicyclo[4.1.0] substrate into 4,5-dihydrobenzo[*b*]furan by using density functional theory (DFT): the heterocycloisomerization of the bicyclo[4.1.0] substrate into 4,5-dihydrobenzo[*b*]furan (model I); the heterocycloisomerization of the bicyclo[4.1.0] substrate into 4,5-dihydrobenzo[*b*]furan without NEt_3 (model II); the heterocycloisomerization of the bicyclo[4.1.0] substrate into 4,5-dihydrobenzo[*b*]furan without $W(CO)_5$ (model III); the heterocycloisomerization of the bicyclo[4.1.0] substrate into 4,5-dihydrobenzo[*b*]furan without $W(CO)_5$ and NEt_3 (model IV), as shown in Scheme 2. This work could provide insight into the cycloisomerization mechanism of the bicyclo[4.1.0] substrate and the role of $W(CO)_5$ and NEt_3 in the reaction and supply a guideline to design novel tungsten complex catalysts with higher performance.

RESULTS AND DISCUSSION

To explore how the bicyclo[4.1.0] substrate isomerizes into 4,5-dihydrobenzo[*b*]furan, and what role $W(CO)_5$ and NEt_3 play in the reaction, four computational models are comparatively discussed as follows.

Heterocycloisomerization of the Bicyclo[4.1.0] Substrate into 4,5-Dihydrobenzo[*b*]furan (Model I). Referring to the experimental proposals, this reaction successfully resulted in the binding of $W(CO)_5$ to the triple bond of bicyclo[4.1.0]

dx.doi.org/10.1021/jo4017748 | *J. Org. Chem.* 2013, 78, 10812−10820

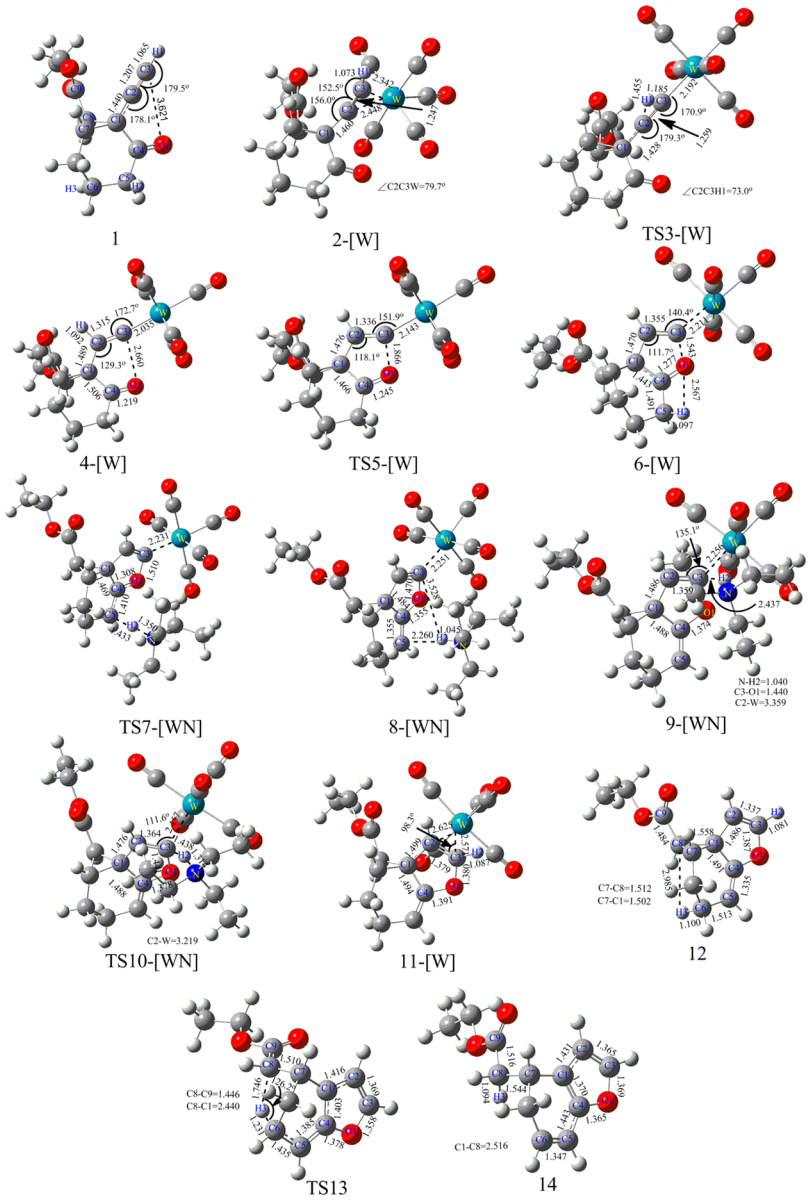

Figure 1. The optimized geometries of model I.

substrate **1** to give the metal complexes **2**-[**W**], the hydrogen transfer in **2**-[**W**] to form metallovinylidene **4**-[**W**] (H1 transfer from C3 to C2), the ring closure of **4**-[**W**] (formation of the C3−O1 bond) to provide the zwitterionic intermediate **6**-[**W**], the isomerization of **6**-[**W**] into η^2-complex **11**-[**W**] under the assistance of NEt_3 (H2 transfer from C5 to NEt_3 and from NEt_3 to C3), the dissociation of $W(CO)_5$ from **11**-[**W**] to give the tricycle **12**, and the rearrangement of **12** (H3 transfer from C6 to C8) to give the final product **14** (**1**→**2**-[**W**]→**TS3**-[**W**]→**4**-[**W**]→**TS5**-[**W**]→**6**-[**W**]→**TS7**-[**WN**]→ **8**-[**WN**]→**9**-[**WN**]→**TS10**-[**WN**]→**11**-[**W**]→**12**→**TS13**→**14**, model I), as shown in Scheme 2. All the optimized geometries of model I are given in Figure 1, and the energy profile is presented in Figure 2.

From **1** to **2**-[**W**], the C2−C3 distance is elongated from 1.207 to 1.247 Å, and the C1−C2 distance is lengthened from 1.440 to 1.460 Å, indicating that when $W(CO)_5$ binds to the C2−C3 triple bond of the bicyclo[4.1.0] substrate, the C1−C2 and C2−C3 bonds are slightly weakened. This is mainly because the bonding π-electrons of the triple bond are dispersed by the unfilled d-orbital of W(0), and the W(0) can feed back its d-electrons into the antibonding orbital (π^*) of the triple bond. This step is calculated to be exergonic by 4.6 kcal/mol.

From **2**-[**W**] to **TS3**-[**W**], which corresponds to the formation of a metallo vinylidene, the C2−C3 distance is elongated from 1.247 to 1.259 Å, and the C3−W distance is shortened from 2.342 to 2.192 Å. The ∠C2C3H1 angle is decreased from 152.5° to 73.0°, and the ∠C2C3W angle is increased from 79.7° to 170.9°. Clearly, when the H1 atom is transferred from C3 to C2 atom, the $W(CO)_5$ simultaneously rearranges from the coordination to the C2−C3 bond (η^2) to the bonding to the C3 atom (η^1). The NBO charges increase from +0.029*e* to +0.091*e* on the C2 atom, and decrease from −0.195*e* to −0.203*e* on the C3 atom, respectively, indicating that the H1 atom with positive charge is transferred from the C3 to the C2 atom (a proton transfer process). The hybridization of the C3 atom is calculated to change from

dx.doi.org/10.1021/jo4017748 | J. Org. Chem. 2013, 78, 10812−10820

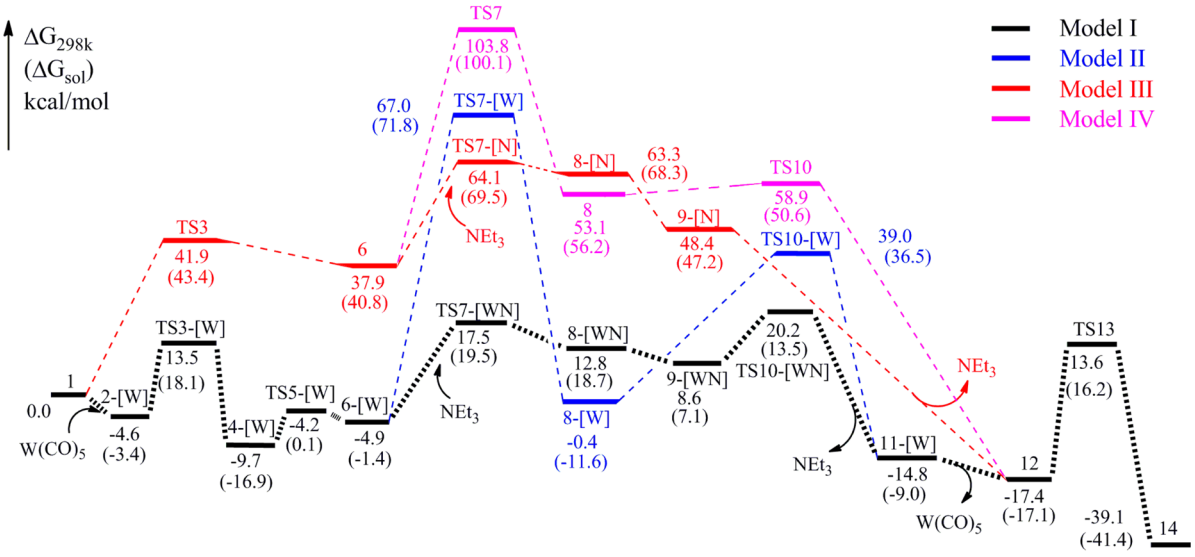

Figure 2. Energy profiles for the cycloisomerization of the bicyclo[4.1.0] substrate into 4,5-dihydrobenzo[*b*]furan.

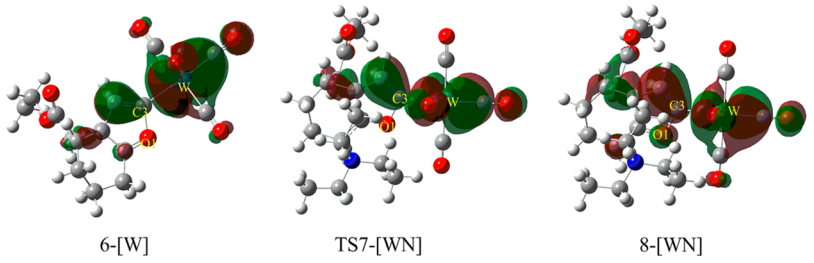

Figure 3. HOMOs of **6**-[**W**], **TS7**-[**WN**], and **8**-[**WN**].

$sp^{1.31}$ to $sp^{1.77}$, also implying that in this process the C2−C3 bond gradually changes from a partial triple bond to a partial double bond. In **4**-[**W**], the distance is 2.035 Å for C3−W (a double bond),[30,31] and 1.315 Å for C2−C3 (a double bond), respectively, supporting that **4**-[**W**] is a typical tungsten−vinylidene complex (metal carbene). This step is calculated to be exergonic by 5.1 kcal/mol with a free energy barrier of 18.1 kcal/mol, which is not difficult to overcome. This is mainly because the formed vinylidene can be stabilized by the $W(CO)_5$ via donating its d-electrons to the carbene.

From **4**-[**W**] to **TS5**-[**W**], corresponding to the ring closure of **4**-[**W**], the C3−O1 distance is shortened from 2.660 to 1.866 Å, the C2−C3 distance is lengthened from 1.315 to 1.336 Å, the C3−W distance is lengthened from 2.035 to 2.143 Å, and the ∠C2C3W angle is narrowed from 172.7° to 151.9°. Clearly, when the O1 atom approaches the C3 atom to form a single bond, the strength of C2−C3 and C3−W bonds decrease. The hybridization of the C3 atom is calculated to change from $sp^{1.36}$ to $sp^{1.56}$, also showing that the C2−C3 bond gradually changes from a partial triple bond to a partial double bond (strength decreased) in the ring closure process. In **6**-[**W**], the C3−O1 distance is 1.543 Å, the C2−C3 distance is 1.355 Å, and the C3−W distance is 2.211 Å, showing that when the ring closure is completed, the C2−C3 bond becomes a typical double bond, and the C3−W bond becomes a typical single bond.[32,33] From **4**-[**W**] to **6**-[**W**], the NBO charges change from −0.534*e* to −0.409*e* on the O1 atom, and from −1.753*e* to −1.760*e* on the W atom, respectively, indicating that in this step the O1 atom gets a partial positive charge and the W atom gets a partial negative charge. These observations, in a sense, support that **6**-[**W**] contains some zwitterionic character. This step is endergonic by 4.8 kcal/mol with a free energy barrier of 5.5 kcal/mol, which is easy to overcome. The driving force of this step mainly originates in the stabilization of the O1 atom with a lone pair of electrons on the carbene C3 atom.

From **6**-[**W**] to **TS7**-[**WN**], the C5−H2 distance is lengthened from 1.097 Å to 1.433 Å, the C4−O1 distance is elongated from 1.277 Å to 1.308 Å, and the C4−C5 distance is shortened from 1.491 Å to 1.410 Å. These show that when the H2 atom migrates from C5 atom to NEt_3, the C4−C5 changes from a single bond into a double bond with the formation of a π-bond, and the C4−O1 changes from a double bond into a single bond with the cleavage of a π-bond. The C3−O1 distance is shortened from 1.543 to 1.510 Å (the bond strength increased). One reason is that when the H2 atom migrates from C5 atom to NEt_3, the O1 atom with a lone pair of electrons can form an extended conjugation system with the metal carbene C3 atom. Another reason is that the transformation of the O1 atom from "O^{+}" in **6**-[**W**] to "O" in **8**-[**WN**] would stabilize the carbene C3 atom. The orbital overlap (HOMO) between the C3 and O1 atoms in **8**-[**WN**] is obviously larger than that in both **TS7**-[**WN**] and **6**-[**W**] (shown in Figure 3), similarly supporting that the strength of the C3−O1 bond gradually increases in this step. The NBO charges change from −0.521*e* to −0.489*e* on the N atom, and from −0.547*e* to −0.581*e* on the C5 atom, implying a proton transfer process. The hybridization of the C5 atom is calculated to decrease from $sp^{2.86}$ to $sp^{2.33}$, also implying that the C4−C5 bond is changing from a single bond to a partial double bond. This step is

dx.doi.org/10.1021/jo4017748 | J. Org. Chem. 2013, 78, 10812−10820

endergonic by 17.7 kcal/mol with a free energy barrier of 22.4 kcal/mol.

The process from **8**-[**WN**] to **9**-[**WN**] is not involved in the formation and breakage of bonds and is calculated to be exergonic by 4.2 kcal/mol, revealing that the $HNEt_3$ group spontaneously approaches the C3 atom. From **9**-[**WN**] to **TS10**-[**WN**], the C3−H2 distance is shortened from 2.437 to 1.438 Å, and the H2−N distance is lengthened from 1.040 to 1.314 Å. The C3−W distance is lengthened from 2.256 to 2.457 Å, the C2−W distance is shortened from 3.359 to 3.219 Å, and the ∠C2C3W angle is decreased from 135.1° to 111.6°. Apparently, when the H2 atom is transferred from NEt_3 to C3 atom, the $W(CO)_5$ simultaneously migrates from bonding to the C3 atom (η^1) to coordination to the C2−C3 double bond (η^2). In other words, the $W(CO)_5$ group on the C3 atom is substituted by the H2 atom and coordinates to the C2−C3 bond again. Compared with the C3−O1 bond strength in **9**-[**WN**], that in **11**-[**W**] obviously increases. This is also attributed to the stable interaction of the O1 atom with the formed carbene C3 atom in this process. This step is calculated to be exergonic by 23.5 kcal/mol with a free energy barrier of 11.6 kcal/mol. The process from **11**-[**W**] to **12**, corresponding to the dissociation of the catalyst $W(CO)_5$, is calculated to be exothermic by 2.6 kcal/mol.

The last step of the $W(CO)_5$-catalyzed heterocycloisomerization is the rearrangement of **12** to give the dihydrobenzofuran derivative **14** (**12**→**TS13**→**14**). The normal-mode analysis and IRC calculation verified that **TS13** consists of the H3 atom motion from the C6 to the C8 atom, connecting **12** with **14**. From **12** to **TS13**, the C6−H3 distance is lengthened from 1.100 to 1.231 Å, the C8−H3 distance is shortened from 2.985 to 1.746 Å, and the C1−C8 distance in the three-membered ring is increased from 1.558 to 2.440 Å. These changes mean that when the H3 atom is transferred from the C6 to the C8 atom, the C1−C8 bond would break. The NBO charges change from −0.491*e* to −0.485*e* on the C6 atom, and −0.340*e* to −0.468*e* on the C8 atom, demonstrating the H3 atom transfer from C6 to C8 atom with a lone pair of electrons through the carbon-conjugated bridge of C6−C5−C4−C1−C8. In other words, this is a [1,5] sigmatropic hydride transfer process. This step is calculated to be exergonic by 21.7 kcal/mol with a free energy barrier of 31.0 kcal/mol.

A comparison of all elementary steps of model I shows that the H3 atom transfer from the C6 to the C8 atom, accompanying the opening of the C1−C7−C8 ring, needs to overcome the highest free energy barrier of 31.0 kcal/mol, being a rate-limiting step in this reaction.

Heterocycloisomerization of the Bicyclo[4.1.0] Substrate into 4,5-Dihydrobenzo[*b*]furan without NEt_3 (Model II). To investigate the role of NEt_3 in the reaction, we designed a computational model without NEt_3. In this model, this reaction successfully resulted in the binding of $W(CO)_5$ to **1** to give **2**-[**W**], the H1 atom transfer in **2**-[**W**] to generate **4**-[**W**], the ring closure of **4**-[**W**] to provide **6**-[**W**], the isomerization of **6**-[**W**] into **11**-[**W**] without NEt_3, the dissociation of $W(CO)_5$ from **11**-[**W**] to give **12**, and the rearrangement of **12** to give **14**, as shown in Scheme 2. The processes of **1**→**2**-[**W**]→**TS3**-[**W**]→**4**-[**W**]→**TS5**-[**W**]→**6**-[**W**] and **11**-[**W**]→**12**→**TS13**→**14** are common between model I and model II and will not be discussed further. The geometries of the other elementary steps in model II are displayed in Figure 4. The corresponding energy profile is also given in Figure 2.

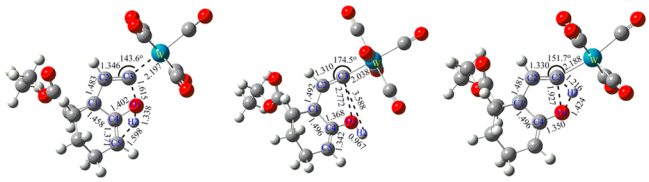

Figure 4. The optimized geometries of model II.

From **6**-[**W**] to **TS7**-[**W**], C4−C5 changes from a single bond (1.491 Å) to a double bond (1.371 Å), C4−O1 gradually changes from a double bond (1.277 Å) to a single bond (1.402 Å) (a typical keto−enol isomerization), and the C3−O1 distance is elongated from 1.543 to 1.615 Å (the bond strength decreased). The main reason is that when **6**-[**W**] isomerizes into its enol form, the C3 atom is stabilized by $W(CO)_5$ but not by the O1 atom. This can be observed from the molecular orbitals. As shown in Figure 5, the orbital overlap (HOMO-1 and HOMO) between the C3 and O1 atoms in **TS7**-[**W**] is obviously less than that between the C3 and W atoms. This process is endergonic by 4.5 kcal/mol with a free energy barrier of 71.9 kcal/mol, which is hardly possible to occur.

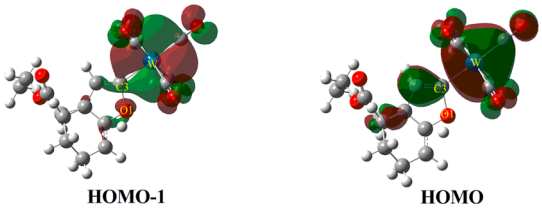

Figure 5. Molecular orbitals of **TS7**-[**W**].

From **8**-[**W**] to **TS10**-[**W**], the H2−O1 distance is increased from 0.967 to 1.424 Å, and the H2−C3 distance is decreased from 3.588 to 1.216 Å. The C2−C3 distance is lengthened from 1.310 to 1.330 Å, the C3−W(0) distance is elongated from 2.038 to 2.188 Å, and the ∠C2C3W angle is decreased from 174.5° to 151.7°. These changes imply that when the H2 atom is transferred from the O1 to the C3 atom, the $W(CO)_5$ simultaneously rearranges from the bonding to the C3 atom (η^1) to the coordination to the C2−C3 double bond (η^2). The C3−O1 distance is shortened from 2.772 to 1.927 Å (the bond strength increased), which is attributed to the formed carbene C3 atom mainly stabilized by the O1 atom but not by $W(CO)_5$. This can also be observed from the molecular orbitals. As shown in Figure 6, on the one hand, the orbital overlap (HOMO-1 and HOMO) between the C3 and O1 atoms in **TS10**-[**W**] is obviously larger than that between the C3 and W atoms. On the other hand, from **8**-[**W**] to **TS10**-[**W**], the orbital overlap between the C3 and W atoms gradually becomes less, while that between the C3 and O1 atoms slowly becomes more. This step is exergonic by 14.5 kcal/mol with a free energy barrier of 39.4 kcal/mol. A comparison of all elementary steps in model II shows that the isomerization of **6**-[**W**] into **8**-[**W**] needs to overcome the highest free energy barrier of 71.9 kcal/mol, being a rate-limiting step.

A comparison between model I and model II shows that when NEt_3 is present, the highest free energy barrier for the isomerization of **6**-[**W**] into **11**-[**W**] is decreased from 71.9 to 22.4 kcal/mol. On the one hand, the O1 atom, which is located in a strained ring system and a delocalized electron-poor system

dx.doi.org/10.1021/jo4017748 | J. Org. Chem. 2013, 78, 10812−10820

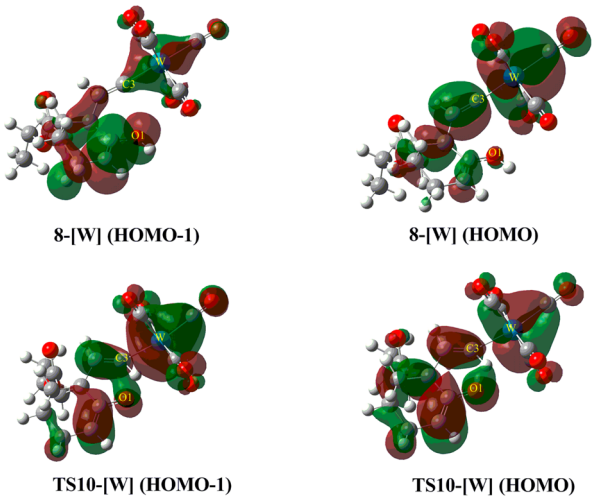

Figure 6. Molecular orbitals of **8**-[**W**] and **TS10**-[**W**].

(O^+), does not easily accept the H2 atom from the C5 atom. On the other hand, the presence of NEt_3 with a lone pair of electrons is favorable for attraction of the H2 atom, and the formed $HNEt_3$ very easily transfers its proton to the C3 atom. In other words, the NEt_3 mainly has an effect in the **6**-[**W**]→**11**-[**W**] stage, in which the NEt_3 can play proton-transfer bridge and proton-adsorption roles.

Heterocycloisomerization of the Bicyclo[4.1.0] Substrate into 4,5-Dihydrobenzo[*b*]furan without $W(CO)_5$ (Model III). To investigate the role of $W(CO)_5$ in the reaction, we designed a computational model without $W(CO)_5$. In this model, this reaction successfully undergoes H1 atom transfer in **1** to give vinylidene **4**, the ring closure of **4** to provide **6**, the isomerization of **6** into **12** with the assistance of NEt_3, and the rearrangement of **12** to give the product **14**, as shown in Scheme 2. The process of **12**→**TS13**→**14** in model III is the same as the corresponding step in model I and will not be discussed further. The geometries of the other elementary steps in model III are displayed in Figure 7. The energy profile is also given in Figure 2.

Many attempts to optimize structure **4** were not successful. The optimization of **4** always gives **6**, implying that **4** is not a real and stable structure. The IRC calculation shows that **TS3** can really connect **1** and **6**. From **1** to **TS3**, the C3−H1 distance is lengthened from 1.065 to 1.240 Å, the C2−H1 distance is shortened from 2.272 to 1.329 Å, and the ∠C2C3H1 angle changes from 179.5° to 64.2°. The C2−C3 distance is elongated from 1.207 to 1.261 Å, and the C3−O1 distance is shortened from 3.621 Å to 3.593 Å. These changes show that when the H1 is transferred from C3 to C2 atom, the C2−C3 bond gradually changes from a triple bond to a double bond, and the C3−O1 bond forms simultaneously, which is in good agreement with the result calculated by K. Morokurna and co-workers.[27] This step (**1**→**TS3**→**6**) is endergonic by 37.9 kcal/mol with a free energy barrier of 41.9 kcal/mol.

A comparison of model I and model III shows that without $W(CO)_5$ the H1 atom transfer in **1** to give **4** and the ring closure of **4** to provide **6** become an elementary process. The highest free energy barrier of this process is increased from 18.1 to 41.9 kcal/mol. Toward understanding this point at the atomic level, the molecular orbitals of the reactants (**1** and **2**-[**W**]) of the two processes are compared, as shown in Figure 8.

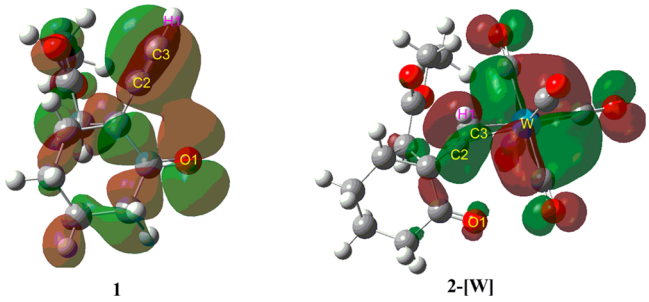

Figure 8. HOMOs of **1** and **2**-[**W**].

In **1**, the H1 atom locates in the middle of two phases of the orbital of the C2−C3 bond (with an orbital nodal surface), being unfavorable to transfer from the C3 to the C2 atom. The HOMO orbital of the C2−C3 bond can overlap with the O1 orbital, showing that the C3 atom is mainly stabilized by the O1 atom. In other words, the formation of the C3−O1 bond is very easy in the catalyst-free process. This would make the H1

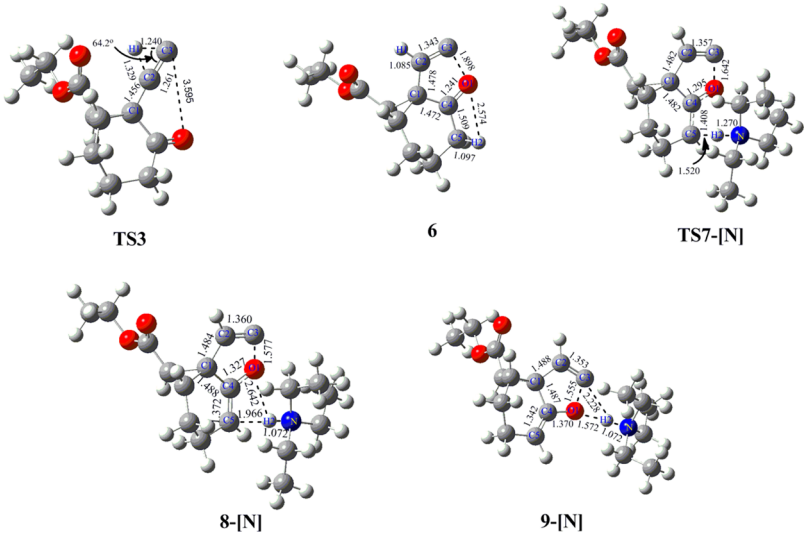

Figure 7. The optimized geometries of model III.

dx.doi.org/10.1021/jo4017748 | J. Org. Chem. 2013, 78, 10812−10820

transfer and the formation of the C3−O1 bond occur in a single step (**1**→**TS3**→**6**). However, in **2**-[**W**] the H1 atom locates in the same phase of the orbital of the C2−C3 bond, which is favorable to transfer from the C3 to the C2 atom. The orbital of the C3 atom overlaps with the $W(CO)_5$ orbital but not the O1 orbital, showing that the C3 atom can be stabilized by $W(CO)_5$ but not the O1 atom. These, in one sense, support the facts that the H1 transfer in **1** to give **4**-[**W**] and the ring closure of **4**-[**W**] to provide **6**-[**W**] take place step-by-step in model I, and the presence of $W(CO)_5$ would promote this process through stabilization of the carbene C3 atom.

From **6** to **TS7**-[**N**], the C5−H2 distance is lengthened from 1.097 to 1.520 Å, the H2−N distance is shortened from 2.493 to 1.270 Å, the C4−O1 distance is elongated from 1.241 to 1.295 Å, and the C4−C5 distance is shortened from 1.509 to 1.408 Å. These changes mean that when the H2 atom is transferred from the C5 to the N atom, the C4−C5 gradually changes from a single bond to a double bond, and C4−O1 gradually changes from a double bond to a single bond. The C3−O1 distance is calculated to shorten from 1.898 to 1.642 Å, revealing that the C3−O1 bond strength is enhanced. Similar to model I, this can be ascribed to the stabilization of the O1 atom on the carbene C3 atom. The molecular orbital analysis gives a similar conclusion, as shown in Figure S1, Supporting Information. This step is endergonic by 10.5 kcal/mol with a free energy barrier of 26.1 kcal/mol. The process from **8**-[**N**] to **9**-[**N**] is not involved in the formation and breakage of the bond and is calculated to be exergonic by 14.9 kcal/mol, revealing a spontaneous process.

Many attempts were made to optimize the transition state **TS10**-[**N**] connecting **9**-[**N**] and **12**; however, they were unsuccessful. To understand this process from the viewpoint of energetics, the relaxed potential energy surface scan from **9**-[**N**] to **12** is performed. As shown in Figure 9, in this process the

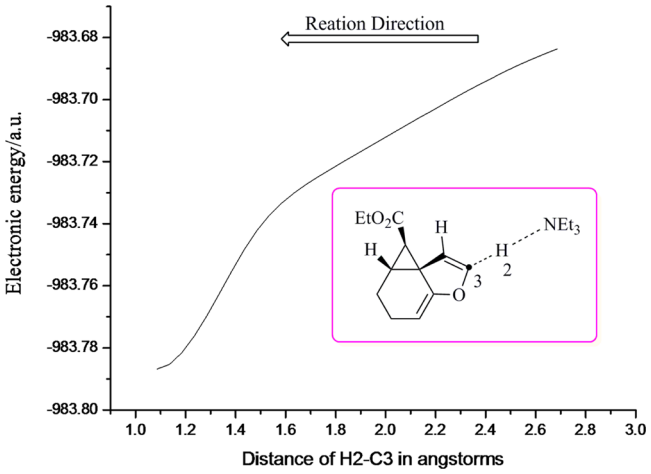

Figure 9. Relative potential energy surface for the H2 migration (**9**-[**N**]→**12**).

energy curve always descends without a clear peak. This means that the H2 transfer from the N to the C3 atom (to form a single bond with the C3 atom) occurs spontaneously.

A comparison of model I and model III shows that the presence of $W(CO)_5$ is slightly favorable for the isomerization of **6** into **12** (the highest free energy barrier: 22.4 vs 26.1 kcal/mol). However, the favorable degree is much less than the case in the presence of NEt_3 (22.4 vs 71.9 kcal/mol). Therefore, $W(CO)_5$ mainly plays a catalytic role in the **1**→**6** stage, in which $W(CO)_5$ can weaken the triple bond of substrate **1** through the back-donation bonding and stabilize the formed carbene C3 atom through its d-electron to the carbene C3 atom.

Heterocycloisomerization of the Bicyclo[4.1.0] Substrate into 4,5-Dihydrobenzo[*b*]furan without $W(CO)_5$ and NEt_3 (Model IV). To better understand the role of $W(CO)_5$ and NEt_3 in the reaction, we designed a computational model without $W(CO)_5$ and NEt_3. In this model, this reaction successfully undergoes the H1 atom transfer in **1** to give vinylidene **4**, the ring closure of **4** to provide **6**, the isomerization of **6** into **12**, the rearrangement of **12** to give the product **14**, as shown in Scheme 2. The process of **1**→**TS3**→**6** and **12**→**TS13**→**14** in model IV is the same as those in model III and will not be discussed further. The geometries of the other elementary steps in model IV are displayed in Figure 10. The corresponding energy profile is also given in Figure 2.

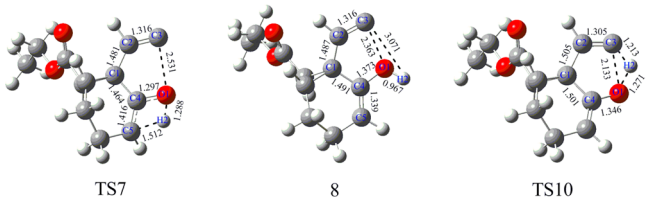

Figure 10. The optimized geometries of model IV.

From **6** to **TS7**, the C5−H2 distance is extended from 1.097 to 1.512 Å, and the O1−H2 distance is shortened from 2.574 to 1.288 Å. The C4−O1 distance is elongated from 1.241 to 1.297 Å, and the C4−C5 distance is shortened from 1.509 to 1.416 Å. These changes show that when the H2 atom is transferred from the C5 to the O1 atom, C4−C5 gradually changes from a single bond to a double bond, and C4−O1 changes from a double bond to a single bond (a keto−enol isomerization). The C3−O1 distance is extended from 1.898 to 2.531 Å (the bond strength decreased), which is because in this model the carbene C3 atom cannot be stabilized by $W(CO)_5$, and the stabilizing effect of the O1 atom on the carbene C3 atom also becomes weak. The molecular orbital analysis gives a similar conclusion, as shown in Figure S2, Supporting Information. This step is endergonic by 15.2 kcal/mol with a free energy barrier of 65.9 kcal/mol. Clearly, without the assistance of $W(CO)_5$ and NEt_3, the keto−enol isomerization process is hardly possible to occur.

From **8** to **TS10** and to **12**, the C3−H2 distance is shortened from 3.071 to 1.213 and to 1.081 Å, the O1−H2 distance is elongated from 0.967 to 1.271 and to 1.081 Å, and the C3−O1 distance is shortened from 2.363 to 2.133 and to 1.387 Å. These changes suggest that when the H2 atom is transferred from the O1 to the C3 atom, the stabilizing effect of the O1 atom on the carbene C3 atom would increase, finally leading to the formation of the C3−O1 bond. The molecular orbital analysis gives a similar conclusion, as shown in Figure S3, Supporting Information. This step is exergonic by 70.5 kcal/mol with a free energy barrier of 5.7 kcal/mol, which is relatively easy to overcome.

A comparison of model I and model IV shows that without $W(CO)_5$, the H1 transfer in **1** to give **4** and the ring closure of **4** to provide **6** become an elementary process. The highest free energy barrier is calculated to increase from 18.1 to 41.9 kcal/mol, which nearly cannot be overcome. The main reason is that

dx.doi.org/10.1021/jo4017748 | J. Org. Chem. 2013, 78, 10812−10820

the formed carbene C3 atom cannot be stabilized by $W(CO)_5$ in model IV. Without NEt_3 serving as a proton-transfer bridge, the isomerization of **6** into **12** is nearly impossible to occur (the free energy barrier is 65.9 kcal/mol).

CONCLUSIONS

In this work, the cycloisomerization mechanism of the bicyclo[4.1.0] substrate into 4,5-dihydrobenzo[*b*]furan and the role of $W(CO)_5$ and NEt_3 in the reaction were systematically investigated by using DFT. Several conclusions were drawn as follows.

A comprehensive comparison of four computational models shows that this reaction is most likely to undergo H1 atom transfer and the ring closure to provide **6**-[**W**] with some zwitterionic character under the assistance of $W(CO)_5$, the isomerization of **6**-[**W**] into **11**-[**W**] under the assistance of NEt_3, the dissociation of $W(CO)_5$ to give the tricycle **12**, and the rearrangement of **12** to give the product **14** (**1**→**2**-[**W**]→**TS3**-[**W**]→**4**-[**W**]→**TS5**-[**W**]→**6**-[**W**]→**TS7**-[**WN**]→ **8**-[**WN**]→**9**-[**WN**] →**TS10**-[**WN**]→**11**-[**W**]→**12**→**TS13**→**14**, model I). The ring closure process is greatly associated with the H1 and H2 transfer processes, because in the H1 atom transfer process the carbene C3 atom is mainly stabilized by $W(CO)_5$, and in the H2 transfer process the carbene C3 atom is mainly stabilized by the O1 atom. The rearrangement of **12** to give **14** needs to overcome the highest free energy barrier of 31.0 kcal/mol, being a rate-limiting step in this reaction.

A comparison of model I and model II shows that the presence of NEt_3 greatly promotes the isomerization of **6**-[**W**] into **11**-[**W**] (the highest free energy barrier: 22.4 vs 71.9 kcal/mol), in which the NEt_3 plays proton-transfer bridge and proton-adsorption roles.

A comparison of model I and model III shows that the presence of $W(CO)_5$ can greatly decrease the free energy barrier for the H1 atom transfer in **1** to give carbene **4**, being favorable for the formation of **6**-[**W**]. This is mainly attributed to stabilizing effect of $W(CO)_5$ on the formed carbene. The presence of $W(CO)_5$ is also slightly favorable for the H2 transfer from C5 to C3 atom (**6**-[**W**]→**11**-[**W**]).

A comparison of model I and model IV shows that without $W(CO)_5$ the H1 atom transfer in **1** to give **4** and the ring closure of **4** to provide **6** is put in an elementary process, and the corresponding free energy barrier becomes very difficult to overcome (41.9 kcal/mol). Without NEt_3 the isomerization of **6** into **12** is almost impossible to occur (the free energy barrier is 65.9 kcal/mol).

The PCM calculations show that the presence of THF solvent causes little change in this reaction, but the overall result is the same as that captured from gas-phase calculations.

COMPUTATIONAL DETAILS

All the calculations were carried out by using Gaussian 09 program suites.[34] The Kohn−Sham density functional theory (DFT) was solved with the B3LYP functional.[35,36] The 6-31G(d,p) basis sets were selected for all nonmetal atoms. The relativistic Lanl2dz effective core potential (ECP) was used for tungsten. The tungsten was modified Lanl2dz, in which the secondary outer p functions of the standard Lanl2dz basis set were replaced with optimized p functions and an *f* polarization function[37,38] was added. All the geometries of reactants, transition states, intermediates, and products were optimized without any constraint. The harmonic vibrational frequency analysis was employed to judge whether the optimized geometry was a minima or a transition state, and to calculate the zero-point energy and Gibbs free energy. Intrinsic reaction coordinate (IRC)[39−41] calculation was carried out to validate the connection of each TS to its corresponding reactant and product. Natural bond orbital (NBO)[42−45] calculations were performed to illustrate the charge distribution in the bonding, and the charge transfer in the reaction. To obtain the energy profile more exactly, a single-point energy calculation was performed at the B3LYP/6-311G(2d,p) level for each species. The polarizable continuum model (PCM)[46,47] was utilized to evaluate the influence of the solvent environment (THF) on the reaction.

ASSOCIATED CONTENT

Supporting Information

The electronic energies, the Gibbs free energies, the solvent free energies, and the Cartesian coordinates for all stationary points. This material is available free of charge via the Internet at http://pubs.acs.org.

AUTHOR INFORMATION

Corresponding Author

*Tel/fax: +86-771-3233718. E-mail: jianyiwang@gxu.edu.cn; jlb39203@gxu.edu.cn.

Notes

The authors declare no competing financial interest.

ACKNOWLEDGMENTS

This work is supported by the National Natural Science Foundation of China (no. 21262004) and the key Scientific Research Project of Guangxi Natural Science foundation (no. 2012GXNSFDA053002). The computational resources are partly provided by Multifunction Computer Center of Guangxi University.

REFERENCES

(1) Ohkawa, S.; Fukatsu, K.; Miki, S.; Hashimoto, T.; Sakamoto, J.; Doi, T.; Nagai, Y.; Aono, T. *J. Med. Chem.* **1997**, *40*, 559−573.
(2) Pieters, L.; Dyck, S. V.; Gao, M.; Bai, R.; Hamel, E.; Vlietinck, A.; Lemière, G. *J. Med. Chem.* **1999**, *42*, 5475−5481.
(3) Engler, T. A.; LaTessa, K. O.; Iyengar, R.; Chai, W.; Agrios, K. *Bioorg. Med. Chem.* **1996**, *4*, 1755−1769.
(4) Clark, D. A.; Goldstein, S. W.; Volkmann, R. A.; Eggler, J. F.; Holland, G. F.; Hulin, B.; Stevenson, R. W.; Kreutter, D. K.; Gibbs, E. M.; Krupp, M. N.; Merrigan, P.; Kelbaugh, P. L.; Andrews, E. G.; Tickner, D. L.; Suleske, R. T.; Lamphere, C. H.; Rajeckas, F. J.; Kappeler, W. H.; McDermott, R. E.; Hutson, N. J.; Johnson, M. R. *J. Med. Chem.* **1991**, *34*, 319−325.
(5) Shi, G. Q.; Dropinski, J. F.; Zhang, Y.; Santini, C.; Sahoo, S. P.; Berger, J. P.; MacNaul, K. L.; Zhou, G.; Agrawal, A.; Alvaro, R.; Cai, T.; Hernandez, M.; Wright, S. D.; Moller, D. E.; Heck, J. V.; Meinke, P. T. *J. Med. Chem.* **2005**, *48*, 5589−5599.
(6) Ward, R. S. *Nat. Prod. Rep.* **1995**, *12*, 183−205.
(7) Kerns, M. L.; Conroy, S. M.; Swenton, J. S. *Tetrahedon Lett.* **1994**, *35*, 7529−7532.
(8) Wang, S.; Gates, B. D.; Swenton, J. S. *J. Org. Chem.* **1991**, *56*, 1979−1981.
(9) Zalkow, L. H.; Ghosal, M. *J. Org. Chem.* **1969**, *34*, 1646−1650.
(10) Togo, H.; Kikuchi, O. *Tetrahedron Let.* **1988**, *29*, 4133−4134.
(11) Kurosawa, W.; Kobayashi, H.; Kan, T.; Fukuyama, T. *Tetrahedron* **2004**, *60*, 9615−9628.
(12) Juhász, L.; Dinya, Z.; Antus, S.; Gunda, T. E. *Tetrahedron Lett.* **2000**, *41*, 2491−2494.
(13) Li, W. S.; Guo, Z.; Thornton, J.; Katipally, K.; Polniaszek, R.; Thottathil, J.; Vu, T.; Wong, M. *Tetrahedron Lett.* **2002**, *43*, 1923−1925.
(14) Gabriele, B.; Mancuso, R.; Salerno, G. *J. Org. Chem.* **2008**, *73*, 7336−7341.
(15) Ghosh, A. K.; Cheng, X.; Zhou, B. *Org. Lett.* **2012**, *14*, 5046−5049.

(16) Itoh, T.; Kawai, K.; Hayase, S.; Ohara, H. *Tetrahedron Lett.* **2003**, *44*, 4081−4084.
(17) Zhu, J.; Price, B. A.; Zhao, S. X.; Skonezny, P. M. *Tetrahedron Lett.* **2000**, *41*, 4011−4014.
(18) Szlosek-Pinaud, M.; Diaz, P.; Martinez, J.; Lamaty, F. *Tetrahedron* **2007**, *63*, 3340−3349.
(19) Youn, S. W.; Eom, J. I. *J. Org. Chem.* **2006**, *71*, 6705−6707.
(20) Hashmi, A. S. K.; Rudolph, M.; Bats, J. W.; Frey, W.; Rominger, F.; Oeser, T. *Chem.—Eur. J.* **2008**, *14*, 6672−6678.
(21) Natori, Y.; Tsutsui, H.; Sato, N.; Nakamuma, S.; Nambu, H.; Shiro, M.; Hashimoto, S. *J. Org. Chem.* **2009**, *74*, 4418−4421.
(22) Tsui, G. C.; Tsoung, J.; Dougan, P.; Lautens, M. *Org. Lett.* **2012**, *14*, 5542−5545.
(23) Pelly, S. C.; Govender, S.; Fernandes, M. A.; Schmalz, H.; Koning, C. B. *J. Org. Chem.* **2007**, *72*, 2857−2864.
(24) Fisher, E. L.; Wilkerson-Hill, S. M.; Sarpong, R. *J. Am. Chem. Soc.* **2012**, *134*, 9946−9949.
(25) Sordo, T.; Campomanes, P.; Diéguez, A.; Rodríguez, F.; Fañanás, F. J. *J. Am. Chem. Soc.* **2005**, *127*, 944−952.
(26) Zhu, J.; Jia, G.; Lin, Z. *Organometallics* **2006**, *25*, 1812−1819.
(27) Sheng, Y.; Musaev, D. G.; Reddy, K. S.; McDonald, F. E.; Morokuma, K. *J. Am. Chem. Soc.* **2002**, *124*, 4149−4157.
(28) Lafrance, M.; Gorelsky, S. I.; Fagnou, K. *J. Am. Chem. Soc.* **2007**, *129*, 14570−14571.
(29) Ando, K.; Kitamura, M.; Miura, K.; Narasaka, K. *Org. Lett.* **2004**, *6*, 2461−2463.
(30) Youinou, M. T.; Kress, J.; Fischer, J.; Aguero, A.; Osborn, J. A. *J. Am. Chem. Soc.* **1988**, *110*, 1488−1493.
(31) Casey, C. P.; Burkhardt, T. J.; Bunnell, C. A.; Calabrese, J. C. *J. Am. Chem. Soc.* **1977**, *99*, 2127−2134.
(32) Evans, S. V.; Legzdins, P.; Rettig, S. J.; Sanchez, L.; Trotter, J. *Organometallics* **1987**, *6*, 7−9.
(33) Koloski, T. S.; Carroll, P. J.; Berry, D. H. *J. Am. Chem. Soc.* **1990**, *112*, 6405−6406.
(34) Frisch, M. J.; Trucks, G. W.; Schlegel, H. B.; Scuseria, G. E.; Robb, M. A.; Cheeseman, J. R.; Scalmani, G.; Barone, V.; Mennucci, B.; Petersson, G. A.; Nakatsuji, H.; Caricato, M.; Li, X.; Hratchian, H. P.; Izmaylov, A. F.; Bloino, J.; Zheng, G.; Sonnenberg, J. L.; Hada, M.; Ehara, M.; Toyota, K.; Fukuda, R.; Hasegawa, J.; Ishida, M.; Nakajima, T.; Honda, Y.; Kitao, O.; Nakai, H.; Vreven, T.; Montgomery, J. A., Jr.; Peralta, J. E.; Ogliaro, F.; Bearpark, M.; Heyd, J. J.; Brothers, E.; Kudin, K. N.; Staroverov, V. N.; Keith, T.; Kobayashi, R.; Normand, J.; Raghavachari, K.; Rendell, A.; Burant, J. C.; Iyengar, S. S.; Tomasi, J.; Cossi, M.; Rega, N.; Millam, J. M.; Klene, M.; Knox, J. E.; Cross, J. B.; Bakken, V.; Adamo, C.; Jaramillo, J.; Gomperts, R.; Stratmann, R. E.; Yazyev, O.; Austin, A. J.; Cammi, R.; Pomelli, C.; Ochterski, J. W.; Martin, R. L.; Morokuma, K.; Zakrzewski, V. G.; Voth, G. A.; Salvador, P.; Dannenberg, J. J.; Dapprich, S.; Daniels, A. D.; Farkas, O.; Foresman, J. B.; Ortiz, J. V.; Cioslowski, J.; Fox, D. J. *Gaussian 09, Revision C. 01*; Gaussian, Inc., Wallingford, CT, 2010.
(35) Becke, A. D. *J. Chem. Phys.* **1993**, *98*, 5648−5652.
(36) Lee, C.; Yang, W.; Parr, R. G. *Phys. Rev. B* **1988**, *37*, 785−789.
(37) Ehlers, A. W.; Böhme, M.; Dapprich, S.; Gobbi, A.; Höllwarth, A.; Jonas, B.; Köhler, K. F.; Stegmann, R.; Veldkamp, A.; Frenking, G. *Chem. Phys. Lett.* **1993**, *208*, 111−114.
(38) Couty, M.; Hall, M. B. *J. Comput. Chem.* **1996**, *17*, 1359−1370.
(39) Gonzalez, C.; Schlegel, H. B. *J. Chem. Phys.* **1990**, *94*, 5523−5527.
(40) Fukui, K. *Acc. Chem. Res.* **1981**, *14*, 363−368.
(41) Gonzalez, C.; Schlegel, H. B. *J. Chem. Phys.* **1989**, *90*, 2154−2161.
(42) Reed, A. E.; Curtiss, A.; Weinhold, F. *Chem. Rev.* **1988**, *88*, 899−926.
(43) Gonzalez, C.; Schlegel, H. B. *J. Phys. Chem.* **1990**, *94*, 5523−5527.
(44) Reed, A. E.; Weinstock, R. B.; Weinhold, F. *J. Chem. Phys.* **1985**, *83*, 735−746.
(45) Glendening, E. D.; Landis, C. R.; Weinhold, F. *Wiley Interdiscip. Rev.: Comput. Mol. Sci.* **2012**, *2*, 1−42.
(46) Cossi, M.; Barone, V.; Cammi, R.; Tomasi, J. *Chem. Phys. Lett.* **1996**, *255*, 327−335.
(47) Miertuš, S.; Scrocco, E.; Tomasi, J. *J. Chem. Phys.* **1981**, *55*, 117−129.